Structural and dynamical properties of zinc-blende GaN, AlN, BN, and their (110) surfaces

H. M. Tütüncü,[1] S. Bağci,[1] G. P. Srivastava,[2] A. T. Albudak,[1] and G. Uğur[3]
[1]*Sakarya Üniversitesi, Fen-Edebiyat Fakültesi, Fizik Bölümü, Mithatpasa, 54100, Adapazari, Turkey*
[2]*School of Physics, University of Exeter, Stocker Road, Exeter EX4 4QL, United Kingdom*
[3]*Gazi Üniversitesi, Fen-Edebiyat Fakültesi, Fizik Bölümü, Teknikokullar, Ankara, Turkey*
(Received 21 September 2004; revised manuscript received 10 February 2005; published 9 May 2005)

Structural and dynamical properties of the zinc-blende bulk phase and the (110) surface of the nitride materials GaN, AlN and BN have been studied by employing an *ab initio* pseudopotential method and a linear response scheme, within the generalized gradient approximation. Trends in surface atomic geometry and energetic locations of surface phonon modes across the nitrides have been discussed. The present *ab initio* results for surface phonons have been compared and contrasted with recently published results obtained from the application of an adiabatic bond charge model, providing thereby a further assessment of the latter scheme for surface lattice dynamics.

DOI: 10.1103/PhysRevB.71.195309 PACS number(s): 68.35.Ja, 63.20.Dj, 68.35.Bs

I. INTRODUCTION

III-N semiconductors have attracted a lot of attention recently, since they are promising materials for light emitting optoelectronic devices in the green and blue color spectrum.[1] These materials are potentially good for protective coatings due to their hardness, high melting point and high thermal conductivity. Current activities in optoelectronic devices have led to significant interest in studies of structural and electronic properties in both wurtzite[2–6] and zinc, blende[4,7–19] phases of III-N semiconductors. Recently, the lattice dynamics of the zinc-blende and wurtzite phases of III-N has been studied using the *ab initio* pseudopotential method[20–25] and an adiabatic bond-charge model.[26,27] On the experimental side, Raman spectroscopy[28–33] has been used to obtain the zone-center phonon frequencies of these materials. This technique has the disadvantage that it can measure only the phonons with small wave vectors. Recently, the lattice dynamics of wurtzite AlN and GaN has been investigated by inelastic x-ray scattering.[34,35] An accurate determination of phonon dispersion curves is important in studies of a wide variety of physical properties of solids, such as specific heat, thermal expansion, electron-phonon interaction, and lattice thermal conduction.

Recently, the atomic geometry and electronic structure of the (110) surface of GaN, AlN and BN have attracted attention.[17,19,36–41] The atomic and electronic structures of these surfaces have been investigated using an *ab initio* pseudopotential method.[17,19,40] However, to the best of our knowledge, only an adiabatic bond-charge model (BCM) has been applied to investigate the lattice dynamics of these surfaces.[42] In order to reconfirm the results obtained from the BCM, or otherwise, it is important to present a systematic study of the lattice dynamics of these surfaces by employing an *ab initio* theoretical technique.

The objective of this paper is to employ the *ab initio* pseudopotential method and the density functional theory, within a generalized gradient approximation, to obtain structural properties of the cubic phase of GaN, AlN and BN and to provide a comparison with previous calculations and experimental data in the literature. This is followed by the application of a linear response scheme for the calculation of phonon dispersion curves. The work on the bulk materials is followed by studies of the (110) surface of these materials. In particular, we aim to provide a systematic study of the trend in the relaxed geometry of the top surface layers across these nitrides, and comment on differences with non-nitride surfaces. The presently calculated surface lattice dynamical results are compared and contrasted with the previously reported BCM results.[42] In addition, we point out surface phonon features which are obtained for III-N(110) but not for non-nitride III-V(110) surfaces.

II. THEORY

We use a first-principles pseudopotential method based on the density functional theory. The pseudopotentials for Al, Ga, B and N atoms are generated according to the scheme of Troullier and Martins.[43] Besides the valence electrons, the semicore Ga 3*d* states are treated following a nonlinear core correction scheme. The density functional theory has been implemented within a generalized gradient approximation, using the Perdew-Burke-Ernzerhof method.[44] A basis set containing all plane waves up to the cutoff energy of 40 Ry for AlN (or BN) and 60 Ry for GaN has been used. In order to perform accurate Brillouin zone integrations for bulk AlN, GaN and BN, we use ten special **k** points within the irreducible part of the bulk Brillouin zone. For the vibrational properties of these materials, we have applied the density functional perturbation theory scheme within the pseudopotential theory, using the pwscf computer code.[45,46] The dynamical matrices have been computed on a $4\times4\times4$ **q**-point mesh, and a Fourier interpolation has been used to obtain complete phonon dispersion curves of these materials.

For surface calculations, we use a supercell method to solve the Kohn-Sham equations self-consistently for electronic and ionic degrees of freedom. The energy cutoff was the same as for the bulk calculations, but the surface Brillouin zone was sampled by six special **k** points. The unit cell along [110] was 11 atomic layers thick, with a vacuum layer equivalent to at least 4 atomic layers. All atoms were allowed

TABLE I. Lattice constant a, bulk modulus B, the pressure derivative of bulk modulus B′, macroscopic dielectric tensor ε_∞ and Born effective charge Z^B of zincblende GaN, AlN and BN. The presently calculated results are compared with other theoretical and experimental data.

III-N	a (Å)	B (Mbar)	B′ (Mbar)	ε_∞	Z^B
GaN	4.46	2.00	4.42	5.95	2.68
Calculated (Ref. 17)	4.43	2.38			
Calculated (Refs. 21,24)	4.46	1.95	3.94	5.41	2.65
Experimental (Refs. 13,15)	4.50	1.90			
Experimental (Ref. 14)				5.30	
AlN	4.36	1.94	3.83	4.50	2.54
Calculated (Ref. 3)	4.32	2.15	4.6		
Calculated (Ref. 19)	4.35	1.86			
Calculated (Refs. 20,24)	4.34	2.09	3.30	4.46	2.56
Experimental (Ref. 7)				4.68	
Experimental (Refs. 13,15)	4.38	2.02			
BN	3.58	3.80	3.56	4.51	1.92
Calculated (Ref. 17)	3.60	3.21			
Calculated (Refs. 20,24)	3.60	4.01	3.6	4.54	1.93
Experimental (Ref. 8)	3.62	3.69	4.0		
Experimental (Ref. 10)				4.46	

to relax into their minimum energy configuration, except for the atoms in the middle of slab which were kept frozen. We calculated dynamical matrices at five q points along each of the principal symmetry directions Γ-X and Γ-X'. Phonon modes were then calculated at an arbitrarily large number of q points along these directions by employing a one-dimensional Fourier transform.[46]

III. RESULTS

A. Bulk

1. Structural properties

The total energy of the zincblende phase of the III-N materials has been calculated for different values of the lattice constant parameter and fitted to Murnaghan's equation state[47] in order to obtain the equilibrium lattice constant a, bulk modulus B and pressure derivative of bulk modulus B′. The calculated static properties (a, B and B′) are given in Table I. In general, our results are in good agreement with avaliable experimental[7,8,10,13–15] and theoretical results.[3,17,19–21,24] In particular, the calculated bulk lattice constant values of 3.58 Å, 4.36 Å and 4.46 Å for BN, AlN and GaN compares very well with experimental values of 3.62 Å,[8] 4.38 Å[13,15] and 4.50 Å.[13,15] In this table, we also report the calculated values of the effective charges and dielectric constants. The dielectric constant is found to be 5.95 for GaN, 4.50 for AlN and 4.51 for BN which can be compared with experimental findings at 5.30,[14] 4.68,[7] and 4.46.[10] Moreover, our calculated Born effective charge values for these materials show good agreement with previous *ab initio* calculations.[20,21,24]

2. Phonon dispersion curves and density of states

The phonon band structures and the corresponding density of states for GaN, AlN and BN are plotted in Fig. 1. The calculated results for all these materials are shown by solid curves while experimental data (closed squares) are taken from Ref. 33 for AlN, Ref. 30 for GaN and Ref. 12 for BN. In this figure, we have also compared our results with previous theoretical calculations: open circles for BCM results[26] and closed triangles for previous *ab initio* results.[24] In general, our results compare very well with these previous theoretical[24,26] and experimental findings.[12,30,33] The general shape of phonon dispersion curves in GaN and AlN are similar to each other. However, there is a large energy gap between acoustic and optical phonons for GaN due to heavy Ga atoms. Second, transverse optic (TO) phonon modes for AlN show the flatness along all high symmetry directions. Due to this flatness, we have observed a very sharp peak in the phonon density of states of AlN. On the other hand, the longitudinal optic (LO) phonon modes for GaN show a very small dispersion along the Γ-X and Γ-L directions. As a result of this, there is a sharp peak in the phonon density states of GaN which is characterized by LO phonon modes. The phonon spectrum of BN is a very different from those of AlN and GaN due-to nearly equal masses of B and N atoms. As can be seen from Fig. 1, there is no clear gap between acoustic and optical phonon modes for BN. The dispersion of LO phonon modes in BN is similar to the dispersion of LO phonon modes in AlN along the main symmetry directions. Thus, there is no sharp peak due to LO phonon modes in the phonon density of states. Moreover, the transverse acoustic (TA) branches for this material are not flat close to the zone edges and thus there is no clear peak due to these phonons in the phonon density of states.

For all the materials, the longitudinal acoustic (LA) phonon mode is characterized by the motion of heavier atoms at the X point. We find that this phonon mode scales almost linearly with $1/a.M^{1/2}_{\text{heavy atom}}$, where a is the cubic lattice constant [see Fig. 2(a)]. At this **q** point, the LO phonon mode

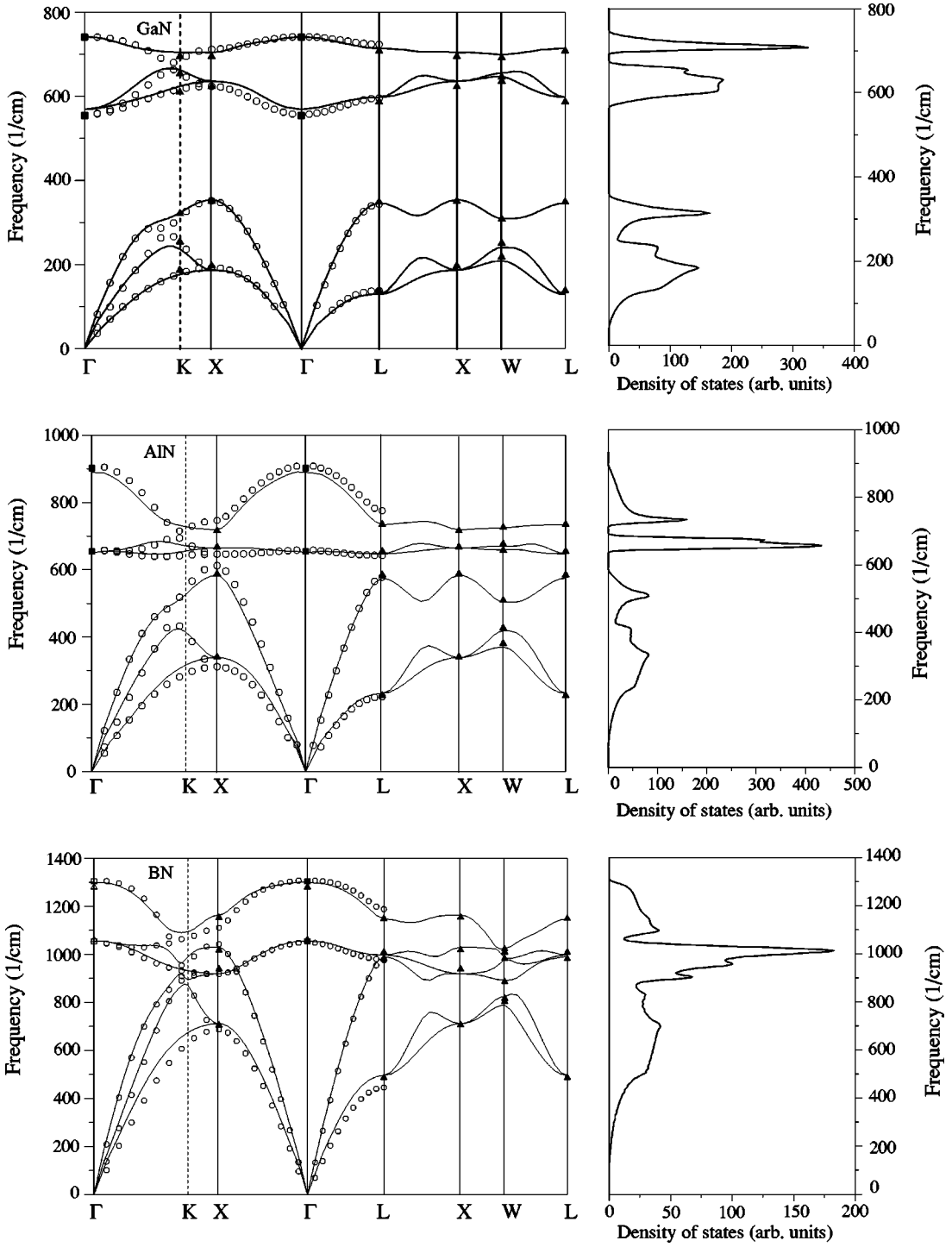

FIG. 1. Calculated phonon dispersions and density of states for GaN, AlN and BN. Experimental data are denoted by closed squares (from Ref. 30 for GaN, Ref. 33 for AlN and Ref. 12 for BN) while previous theoretical calculations are shown by open circles for the adiabatic bond-charge model results (Ref. 26) and closed triangles for previous *ab initio* results (Ref. 24).

originates from the motion of the lighter atom for all considered materials. Thus, the energy difference in the LO phonon mode of GaN, AlN and BN can be directly related to the difference in the lattice constant as well as the difference in the mass of the lighter atom between these materials. Thus, we can calculate the LO phonon mode of BN from the corresponding phonon mode of AlN and GaN by using the relation

$$\omega(\mathrm{LO})_{\mathrm{BN}} = \frac{a(\mathrm{AlN}\ or\ \mathrm{GaN})}{a(\mathrm{BN})} \sqrt{\frac{M_N}{M_B}}\, \omega(\mathrm{LO})_{\mathrm{AlN\ or\ GaN}}. \quad (1)$$

The above relation can be used without any consideration of masses for AlN and GaN because the lighter mass in these materials is of the same atom (N). As can be seen from Fig. 1, for both AlN and GaN, the LO mode frequency is almost

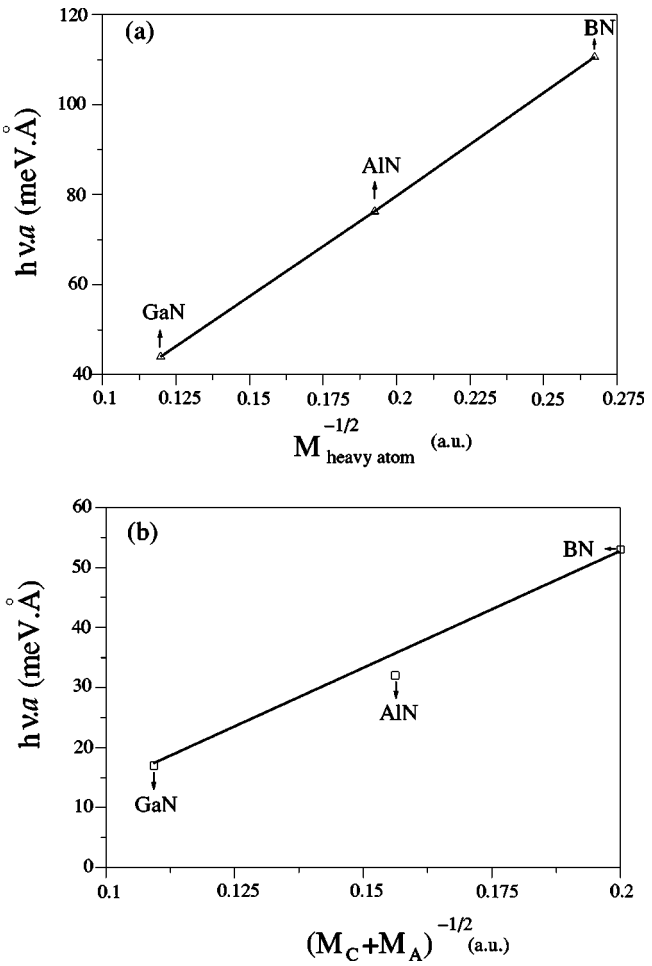

FIG. 2. (a) Variation of the LA phonon energy at the X point with respect to the lattice constant and heavier basis mass. (b) The variation of the TA phonon energy at the L point with respect to the lattice constant and heavier basis mass.

the same at the X and L points. Thus, the same relationship can be expected for the LO phonon modes in GaN and AlN at the L point. Finally, the atomic vibrational pattern of the TA phonon mode at the L point is pictured by a mixture of the motion of group III atoms and N atoms. The effect of the difference in the total mass and of the difference in the lattice constant on the TA phonon mode at the L point is also shown in Fig. 2(b).

B. (110) surfaces of GaN, AlN and BN

1. Structural properties

The atomic relaxation pattern on the III-N(110) surfaces is similar to that for all studied zincblende(110) surfaces:[48] at the top-layer group-III surface atoms relax inward, while the N atoms are shifted above the surface. The driving mechanism of this atomic rearrangement is the desire for sp^2 bonding configuration of cation surface atoms with their group-V neighbors. On the other hand, the first layer anions prefer to be situated in a *p*-bonding configuration with their group-III neighbors. This leads to a rotation of the surface chains by a tilt angle ω_1 as shown in Fig. 3. Table II summarizes our

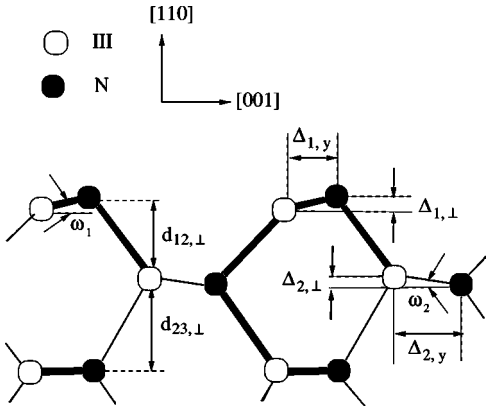

FIG. 3. Schematic relaxed side view of III-N(110).

results for the relaxation parameters of the (110) surfaces of GaN, AlN and BN, together with previous theoretical results.[19,36,40] In general, the calculated parameters are in good agreement with a recent *ab initio* calculation by Miotto *et al.*[19] Our calculated tilt angle of the first layer is found to be 12.0 deg for AlN(110), 16.0 deg for GaN(110) and 17.9 deg for BN(110). These values compare well with the work of Miotto *et al.*[19] who reported the tilt angle of 11.9 deg for AlN(110), 17.5 deg for GaN(110) and 16.6 deg for BN(110).

It is interesting to compare and contrast the geometrical characteristics of the III-N(110) surfaces with non-nitride zincblende(110) surfaces. First, for non-nitride zincblende(110) the surface tilt angle ω_1 assumes a nearly constant value in the range 28 deg $< \omega_1 <$ 32 deg.[48] A similar result is obtained for the III-N(110) surfaces, *albeit* with a smaller value of the mean rotation angle: 12 deg $< \omega_1 <$ 18 deg. Second, the surface buckling $\Delta_{1,\perp}$ increases almost monotonically with the bulk lattice constant *a* for both non-nitride and nitride surfaces. The relationship $\Delta_{1,\perp} \propto a$ is an empirical one, first proposed by Duke,[49] and is based on the implicit assumption of bond-length conservation at the surface. While the surface bond length is nearly conserved for non-nitride(110) surfaces, from Table II it is clear that the III-N surface bond length contracts in the range 4%–7% compared to its bulk value. This difference in the characteristics of the surface bond length between the non-nitride and nitride surfaces spoils the empirical relationship $\Delta_{1,\perp} \propto a$ when we try to make a generalization across all zincblende(110) surfaces. The theoretical investigations by Miotto *et al.*[19] suggests that a better empirical relationship is $\Delta_{1,\perp} \propto d$, where *d* is the surface bond length, and our results agree with this.

2. Phonons on GaN(110)

In Fig. 4, we display the phonon dispersion curves of the GaN(110) surface along the $\bar{\Gamma}$-$\bar{X}$ and $\bar{\Gamma}$-$\bar{X}'$ directions. It is important to note that there are three localized gap phonon states in the acoustic-optical gap range. The lower two of these phonon states are nearly flat along the both symmetry directions, with the energy difference of about 15 meV. We have observed that the highest surface optical phonon mode shows a dispersion along the $\bar{\Gamma}$-$\bar{X}$ direction while it is nearly flat in the other symmetry direction.

TABLE II. Calculated structural parameters and their comparison with previous theoretical calculations for the AlN(110), GaN(110) and BN(110) surfaces. Distances are in Å. $\delta d/d$ represents the fractional reduction in surface bond length compared to the bulk value.

	$\Delta_{1,\perp}$	$\Delta_{2,\perp}$	$\Delta_{1,y}$	$\Delta_{2,y}$	$d_{12,\perp}$	$d_{23,\perp}$	ω_1	ω_2	$\frac{\delta d}{d}$ (%)
AlN									
Present	0.185	0.04	0.87	1.08	1.49	1.59	12.0 deg	2.1 deg	5.7
ab initio (Ref. 36)	0.303				0.891		20.8 deg		
ab initio (Ref. 40)	0.131				0.891		11.6 deg		
ab inito (Ref. 19)	0.182	0.04			1.485		11.9 deg	2.08 deg	
GaN									
Present	0.270	0.040	0.94	1.10	1.511	1.61	16.0 deg	2.10 deg	3.6
ab inito (Ref. 36)	0.315						19.4 deg		
ab inito (Ref. 40)	0.32				1.103		14.3 deg		
ab inito (Ref. 19)	0.281	0.043			1.454		17.5 deg	2.25 deg	
BN									
Present	0.213	0.029	0.66	0.87	1.124	1.3	17.9 deg	1.90 deg	7.4
ab initio (Ref. 36)	0.276						21.7 deg		
ab initio (Ref. 40)	0.187				0.837		15.7 deg		
ab initio (Ref. 19)	0.203	0.027			1.149		16.6 deg	1.75 deg	

The surface phonons at the center of the surface Brillouin zone can be classified according to the irreducible representations of C_s (or m), the point group symmetry of the surface unit cell. Thereby A″ modes describe lattice distortions along the $[1\ \bar{1}\ 0]$, and A′ modes correspond to atomic movements perpendicular to the chain direction. At the zone center, we have found three localized phonon modes with energies of 22.0, 77.4 and 91.7 meV with an A″ character while there are five localized A′ phonon modes with energies of 41.0, 57.0, 68.0, 75.0 and 88.0 meV. These phonon modes can be compared with corresponding previous BCM results[42] with energies of 24.0 and 84.4 meV with an A″ character and 40.1, 62.8, 75.8 and 91.0 meV with an A′ character. The lowest A″ phonon mode obtained from the present *ab initio* calculation is due to a dispersionless branch along the $\bar{\Gamma}$-$\bar{X}$ direction. For this phonon mode, the cation atoms have larger atomic displacements than anionic atoms and thus it can be called a cationic chain mode. The atomic displacement patterns of the

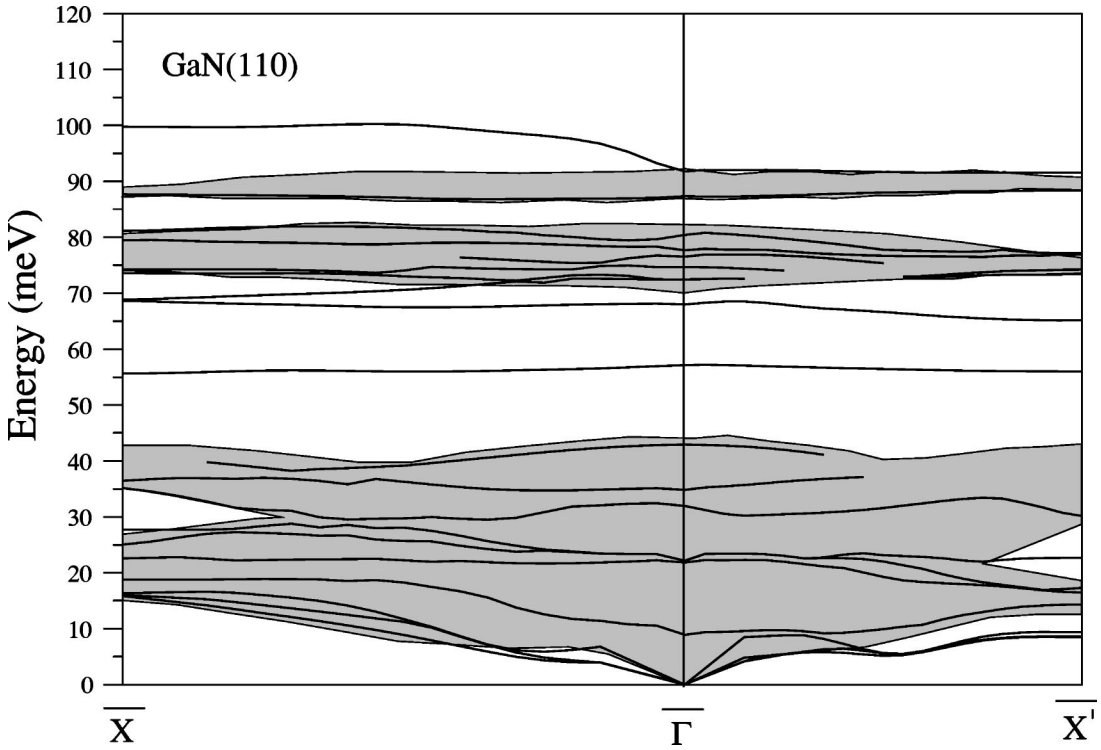

FIG. 4. Surface phonon dispersion curves of GaN(110). The projected bulk phonon dispersion is shown by a hatched region.

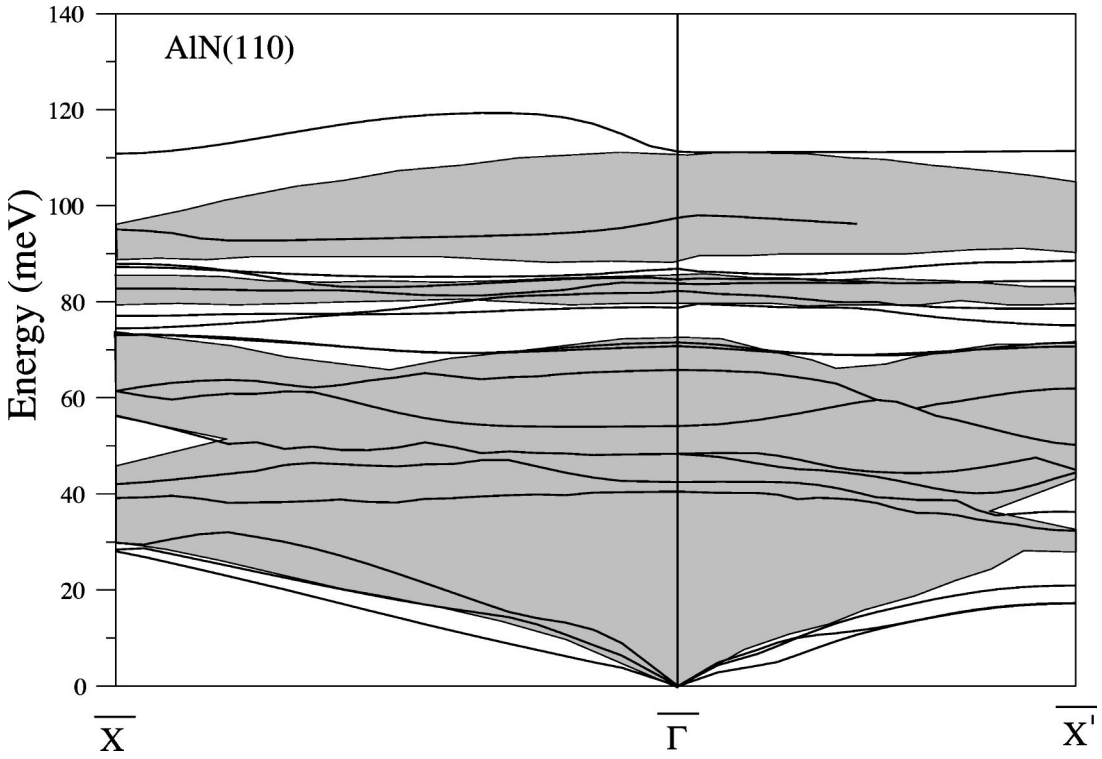

FIG. 5. Phonon spectrum of the AlN(110) surface. The projected bulk phonon dispersion is shown by a hatched region.

second A″ phonon mode has been pictured by vibrations of second layer N atoms. The highest surface optical phonon mode mainly originates from the atomic motion of the first-layer atoms in the zig-zag chain direction, i.e., is an A″ mode. The A′ phonon mode with the lowest energy can be also interpreted as a cationic mode due to large atomic vibrations of second and third layer Ga atoms. The most interesting phonon modes are found in the acoustic and optical phonons gap region. There are two gap phonon modes in this region with energies of 57.0 and 68.0 meV. The lower mode at 57.0 meV has a rotational character and is nearly flat along both the symmetry directions. The energy and atomic displacement character of this phonon mode can be compared with the BCM phonon mode at 62.8 meV.[42] The higher acoustic-optical gap mode is also dispersionless and originates from the vibrations of N atoms in the top three layers. Due to the very large mass difference between Ga and N atoms, the higher energy A′ modes at 75.0 meV and 88.0 meV are also mainly localized on the N atoms.

Surface acoustic waves are found to be localized phonon modes for larger wave vectors along the $\overline{\Gamma}$-$\overline{X'}$ direction. The lowest acoustic phonon mode with energy of 8.5 meV is the Rayleigh wave (RW). The symmetry character of this phonon modes is A′ with in-phase vibrations of surface layer atoms in the [001] direction. The BCM method[42] also predicts the A′ character for this phonon mode but the energy of this mode is 2.5 meV higher than the RW phonon mode from our *ab initio* work. Along the $\overline{\Gamma}$-$\overline{X'}$ direction, we identify a flat branch with an energy of about 23 meV which turns into a localized gap phonon mode close to the $\overline{X'}$ point. In our BCM work,[42] the energy of this phonon mode is found to be 25 meV with a similar polarization character. The acoustic and optical gap region phonon modes are found at 55.9 meV and 65.1 meV. These phonon modes have an A′ polarization character. The second one compares very well with the gap phonon mode at 64.6 meV in our BCM work.[42] Finally, the highest surface optical phonon mode along the $\overline{\Gamma}$-$\overline{X'}$ direction does not change its energy and polarization character. Again, this phonon mode is due to the opposing motion of surface layer atoms in the zig-zag chain direction with energy of 91.5 meV.

The phonon modes along the $\overline{\Gamma}$-$\overline{X}$ direction show a mixture of the A′ and A″ character. The energy of the RW phonon mode is found to be 16 meV which compares very well with the corresponding phonon mode 16.5 meV in our BCM work.[42] The energy locations of the acoustic-optical gap region phonon modes are similar to the corresponding phonon modes at the zone center but their vibrational patterns are different. The lower one at 55.6 meV is generated by motion of first layer Ga atoms in the zig-zag chain direction while the first layer N atoms move in the [110] direction. The higher one at 68.5 meV is an anionic phonon mode with the motion of second layer N atoms in the surface normal direction. Along this direction, the highest surface optical phonon mode shows a large dispersion close to the zone center. However, for large wave vectors, this phonon branch becomes flat with energy of about 100 meV. This phonon mode is also an anionic phonon mode due to the motion of first layer N atoms in the zig-zag chain direction.

3. Phonons on AlN(110)

We show the phonon spectrum of the AlN(110) surface together with the surface projected bulk structure in Fig. 5. For this surface, the lowest surface acoustic mode turn into a

truly localized state along both symmetry directions. The highest optical phonon mode on this surface shows dispersion which is similar to that on the GaN(110) surface. The *ab initio* A′ phonon mode at 40 meV corresponds to a nearly dispersionless state along the $\bar{\Gamma}$-$\bar{X}$ direction. This phonon mode is mainly characterized by opposing motion of first and second layer Al atoms in the surface normal direction. In addition to this A′ mode, we have identified five localized A′ modes with energies of 42.5, 48.5, 54.2, 71.0 and 87.0 meV. The atomic displacement patterns of three phonon modes with energies of 48.5, 54.2 and 87.0 meV includes a rotational character due to the opposing motion of first layer atoms in the surface normal direction. The highest one can be compared with the rotational phonon mode of the BCM model[42] at 90.0 meV. Due to the mass difference between Al and N atoms, this phonon mode includes larger atomic vibrations from the first three layer N atoms. Finally, the highest surface optical phonon mode at 111.0 meV with an A′ character has displacement patterns similar to its corresponding zone-center phonon mode on the GaN(110) surface.

At the $\bar{X}'$ point of the surface Brillouin zone, with the surface phonon wave vector directed along [001], two acoustic phonon frequencies are found to be 17.3 meV and 20.9 meV. These phonon modes have A′ and A″ characters, respectively. These phonon modes are basically drawn out of the bulk acoustic modes, but lie below the bulk phonons due to reduced coordination of surface atoms. The RW phonon mode at 17.3 meV has been placed at 19.3 meV in our BCM calculations[42] with an A′ polarization character. We find that the second acoustic phonon mode is a strongly localized on the first layer atoms due to the vibrations in the zig-zag chain direction. At this symmetry point, we have observed a stomach gap phonon mode at 36.3 meV which is dominated by the motion of top layer atoms with components both in the [110] and [001] directions. The energy of this phonon mode compares very well with the corresponding BCM phonon mode at 38 meV.[42] In agreement with BCM calculations,[42] *ab initio* calculations yield two localized phonon modes in the acoustic and optical phonons gap region with energies of 75.1 meV and 78.0 meV. The lower gap phonon mode includes a bond-stretching character which has been also observed for the corresponding phonon mode at 73.4 meV in our BCM calculations.[42] However, these two phonon modes are also characterized by large atomic vibrations of second and third layer N atoms, respectively. In addition to these gap phonon modes, there are two more gap phonon modes in the bulk optical-optical gap region. The zone-boundary frequencies of these modes are 84.3 meV and 88.5 meV. The first one has an A′ character and is identified as a subsurface layer chain mode with the opposing vibrations of second layer atoms in the zig-zag chain direction. However, the second gap phonon mode is an anionic phonon mode due to large vibrations of first and second layer N atoms perpendicular to the zig-zag chain direction. At this **q** point, the energy and polarization character of the highest surface optical phonon mode is similar to the corresponding phonon mode at the zone center.

We have found that the RW phonon mode at the $\bar{X}$ point comes from the motion of first layer Al atoms in the chain direction while first layer N and second layer Al atoms move perpendicular to the chain direction. The energy of this phonon mode is found to be 28.0 meV which compares very well with the RW phonon mode of the BCM model at 27.0 meV.[42] At this **q** point, we obtain two localized gap phonon modes at energies 74.4 meV and 76.9 meV in the acoustic-optical gap region. The lower is mainly characterized by the motion of second layer atoms with components both in the [110] and [001] directions while the second one is mainly localized on the third layer N atoms. The highest surface frequency includes very large atomic vibration from first layer N atoms in the chain direction while surface layer Al atoms move in the [001] direction with a smaller amplitude. As a result, with increased phonon energies, atomic vibrations of N atoms become very important due to the mass difference between Al and N atoms.

4. Phonons on BN(110)

The phonon dispersion calculated for BN(110) is illustrated in Fig. 6. The highest surface optical phonon mode lies below the bulk phonons along the $\bar{\Gamma}$-$\bar{X}'$ direction. Due to a very small mass difference between cation and anion atoms there is no significant band gap between the acoustic and optical phonon modes. For this surface, the RW phonon mode lies well below the project bulk phonon spectrum along both the symmetry directions. At the zone center, the lowest A′ phonon mode found at 75.0 meV is generated by the opposing motion of the first and second layer atoms in the surface normal direction. We found a bond stretching mode at 117.4 meV and a rotational phonon mode at 139.5 meV. In view of the fact that theoretical estimates have error margins of 2.0 meV, it should be said that the calculated rotational phonon mode compares well with the corresponding BCM phonon mode at 140.0 meV.[42] For this surface, the highest zone-center frequency is observed at 158.0 meV with an A′ polarization character. The surface phonon modes with a group symmetry representation A″ are found at energies 131.0 meV and 150.5 meV. The higher one is a surface layer zig-zag chain mode while the lower-lying mode corresponds to opposing motion of second layer atoms in the zig-zag chain direction.

At the zone edge point $\bar{X}'$, we identify the RW phonon mode at 36.0 meV with an A′ polarization character. This phonon frequency is characterized by displacements of surface layer atoms in the [001] direction. A similar observation has been made in our BCM calculation[42] which places it at 38.0 meV. The second frequency, which is at 42.0 meV, is also an acoustic mode with first layer atoms vibrating in the A″ mode. This frequency is also in very good agreement with the BCM A″ phonon mode at 41.8 meV.[42] The lowest surface optical frequency at 74.0 meV is a stomach gap phonon mode with an A′ character. At this **q** point, we have identified another gap phonon mode at 131.0 meV. This phonon mode has an A″ character and similar displacement patterns to the corresponding zone-center phonon mode at the same energy. Again, the atomic displacement pattern of the highest lying A″ phonon mode at 149.9 meV is similar to a surface layer zig-zag chain mode at the zone center. Finally, the phonon mode at 157.5 meV is A′ phonon mode and

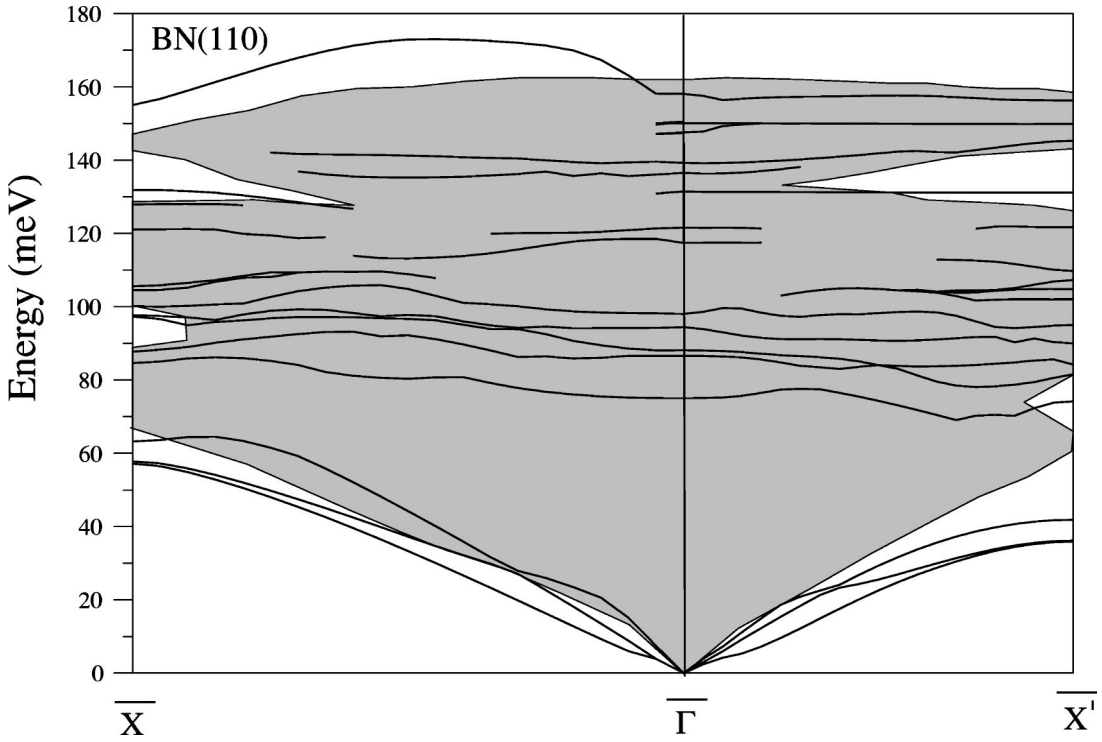

FIG. 6. Phonon spectrum of the BN(110) surface. The projected bulk phonon dispersion is shown by a hatched region.

belongs to the highest surface optical branch.

The BN(110) surface exhibits two surface acoustic phonon modes at $\overline{X}$, as found on the GaN(110) and AlN(110) surfaces. These are predicted at energies of 57.5 meV and 63.2 meV. The polarization character of the RW phonon mode is a quite similar to the RW phonon mode at 57.9 meV in our BCM calculations.[42] Two localized gap phonon modes have been identified with energies 97.7 meV and 132.0 meV at the $\overline{X}$ point. The second one has been placed at 135.0 meV by using the BCM method.[42] Different from the $\overline{X'}$ point, the highest surface optical phonon mode lies above the projected phonon spectrum at this **q** point. In addition to this, the polarization character of this phonon mode includes a large contribution of atomic vibrations from the first-layer B atoms in the zig-zag chain direction while the first-layer N and the second-layer B atoms move with components both in the [110] and [001] directions.

5. Similarities and differences

The most important trends with variations in the mass and lattice constant for the surface phonon modes on GaN(110), AlN(110) and BN(110) surfaces can be observed for the highest surface optical phonon branch along both symmetry directions. This phonon branch is mainly due to opposing motion of first-layer atoms. Thus, the energy locations of the highest surface optical phonon mode can be linked to the differences in the reduced mass and lattice constant of these materials. For example, the average energy along the $\overline{\Gamma}$-$\overline{X}$ and $\overline{\Gamma}$-$\overline{X'}$ directions of this phonon mode shows the ratio 1.20/1.00 for AlN(110) and GaN(110), 1.43/1.00 for BN(110) and AlN(110) and 1.70/1.00 for BN(110) and GaN(110). These values correlate very well with the ratio $a_{bigger}/a_{smaller} \times \sqrt{\mu_{bigger}}/\sqrt{\mu_{smaller}}$, which is 1.23/1.00 for AlN and GaN, 1.47/1.00 for BN and AlN, 1.72/1.00 for BN and GaN, respectively. For all the considered surfaces, the RW phonon mode at the $\overline{X'}$ point is found to lie below the projected bulk phonon spectrum with an A′ polarization character. Due to the mass difference between Ga (or Al) and N atoms, a cationic phonon mode has been identified for GaN(110) and AlN(110) surfaces. Finally, the localized gap phonon modes in the acoustic and optical gap region are only clearly observed for the GaN(110) surface. One of these modes lies in the middle of the acoustic-optical gap region, which can be understood to be due to a heavy cation mass-similar observation has been made for GaP(110), InP(110) and InAs(110) surfaces which also have heavier cation masses.[50,51]

In order to highlight differences and similarities between phonons on nitride surfaces and non-nitride surfaces, we have compared selected surface phonon modes on GaN(110) with the corresponding phonon modes on GaP(110) and InP(110) surfaces[51] at the $\overline{X'}$ point in Table III. Due to the large mass difference between cation and anion atoms, a direct comparison is possible for these surfaces. In general, surface phonon modes on GaN(110) lie higher energies than the corresponding surface phonon modes on these non-nitride surfaces because of smaller reduced-total masses and the lattice constant of GaN. Table III clearly shows that most of the phonon modes on the GaN(110) surface have similar polarization characters with their counterparts on non-nitride surfaces. However, the main difference between lattice dynamics of GaN(110) and non-nitride surfaces has been observed in the polarization character of the highest surface optical phonon mode. This phonon mode has an A″ polariza-

TABLE III. Calculated surface phonons on the GaN(110) surface at the $\overline{X'}$ point and their comparison with those on the GaP(110) and InP(110) surfaces (Ref. 51). Various modes are identified as follows: Rayleigh wave (RW), stomach gap phonon mode (SGPM), first localized gap phonon mode (FLGPM), second localized gap phonon mode (SLGPM) and highest surface optical phonon mode (HSOPM).

Surface	RW	SGPM	FLGPM	SLGPM	HSOPM
GaN(110)	8.50(A′)	23.00(A′)	55.90(A′)	65.10(A′)	91.5(A″)
GaP(110) (Ref. 51)	7.71(A′)	15.91(A′)	37.21(A′)	39.01(A′)	50.35(A′)
InP(110) (Ref. 51)	5.56(A′)	11.55(A′)	34.50(A′)	36.81(A′)	44.75(A′)

tion character for the GaN(110) surface while it is an A′ phonon mode for the non-nitride surfaces. Moreover, this phonon mode is mainly localized on the surface layer atoms while it includes large atomic vibrations from second and third layer atoms for non-nitride surfaces.[50,51] A similar observation has been made for the highest zone-center phonon mode on a GaN(110) surface. In addition to this, this phonon mode also has an A″ character for the AlN(110) surface at the $\overline{\Gamma}$ and $\overline{X'}$ points. However, the polarization character of this phonon mode for BN(110) is different from those for AlN(110) and GaN(110) surfaces. This phonon mode has an A′ character for the BN(110) surface at the zone center and $\overline{X'}$ symmetry points. This can be due to small mass differences between the B and N atoms. As a result of this small mass difference, this surface shows a dynamical behavior similar to that observed for the GaAs(110) surface.[52,53] However, the position of the Al and N atoms in the Periodic Table indicates that the dynamical properties of AlN should be similar to SiC. In one of our works,[54] we have observed that the highest surface optical phonon mode of the SiC(110) surface originates from the opposing motion of first-layer atoms in the zig-zag chain direction with A″ character at the $\overline{\Gamma}$ and $\overline{X'}$ symmetry points.

In general, our *ab initio* results are in agreement with the previous BCM results.[42] However, some differences between phonon calculations obtained from the application of the BCM and *ab initio* methods are inevitable. This difference can be due to a proper treatment in the *ab initio* work of the interatomic force constant and effective charges at the surface layer. The most notable difference between *ab initio* and BCM results lies in the location of the highest surface optical phonon mode. Our *ab initio* work indicates that this phonon mode lies above the bulk continuum along the $\overline{\Gamma}$-$\overline{X}$ direction while the BCM predicts it as resonant with bulk along the same symmetry direction. Another difference has been observed in the gap phonon modes of the GaN(110) surface. In our *ab initio* calculations, two surface-localized phonon states appear in the acoustic-optical gap range while the BCM work reports only one localized phonon mode in this gap region.

IV. SUMMARY

In the first part of this paper, a first-principles study, using a linear-response approach based on the pseudopotential method and the generalized gradient approximation scheme, has been carried out for structural and dynamical properties of zincblende GaN, AlN and BN. The equilibrium lattice constants, bulk modulus and its pressure derivative for all considered III-N are in good agreement with previous theoretical and experimental findings. The effective charges and dielectric constants for all considered III-N are also found to be in good agreement with previous theoretical and experimental results. The obtained phonon dispersion curves for these III-N compare very well with the zone-center Raman measurements and previous theoretical results.

In the second part of this paper, we have investigated the structural properties of the (110) surface of III-N compounds GaN, AlN and BN. The calculated structural parameters for these surfaces are in good agreement with previous *ab initio* calculations. Using our atomic geometry, we calculated the phonon dispersion curves of these surfaces along the $\overline{\Gamma}$-$\overline{X}$ and $\overline{\Gamma}$-$\overline{X'}$ symmetry directions by applying a linear-response approach based on the pseudopotential method. From the phonon dispersion of these surfaces, we have made several observations: first, the highest surface optical phonon branch shows a dispersion along the $\overline{\Gamma}$-$\overline{X}$ direction while it is nearly flat along the other symmetry direction. Second, the acoustic-optical gap phonon modes throughout the surface Brillouin zone are only found for the GaN(110) surface due to a large mass difference between Ga and N atoms. Third, the vibrational pattern of the highest surface optical phonon mode on the BN(110) surface is different from those on the GaN(110) and AlN(110) surfaces. Finally, in agreement with BCM calculations, the energy location of this phonon mode for GaN(110), AlN(110) and BN(110) surfaces can be explained in terms of the differences in the lattice constant and reduced mass.

Although most calculated surface phonon modes compare well with results obtained from recent BCM calculations at the symmetry points, some differences have been observed due to the different physical natures of both models. Although there is an overall agreement between the BCM and the present results, in the present work we highlight the importance of first-principles calculations by pointing out that the energy location and dispersion of some modes obtained from the BCM are found to differ from the first-principles results appreciably.

[1] S. Nakamura, *The Blue Laser Diode-GaN Based Light Emitters and Lasers* (Springer-Verlag, Berlin, 1997).
[2] H. P. Maruska and J. J. Tietjen, Appl. Phys. Lett. **15**, 327 (1969).
[3] P. E. Van Camp, V. E. Van Doren, and J. T. Devreese, Phys. Rev. B **44**, 9056 (1991).
[4] M. van Schilfgaarde, A. Sher, and A. B. Chen, J. Cryst. Growth **178**, 8 (1997).
[5] K. Parlinski and Y. Kawazoe, Phys. Rev. B **60**, 15 511 (1999).
[6] V. J. Keast, A. J. Scott, M. J. Kappers, C. T. Foxon, and C. J. Humphreys, Phys. Rev. B **66**, 125319 (2002).
[7] L. Akasaki and M. Hashimoto, Solid State Commun. **5**, 851 (1967).
[8] E. Knittle, R. M. Wentzcovitsch, R. Jeanloz, and M. L. Cohen, Nature (London) **337**, 349 (1989).
[9] Y. N. Xu and W. Y. Ching, Phys. Rev. B **48**, 4335 (1993).
[10] N. E. Christensen and I. Gorczyca, Phys. Rev. B **50**, 4397 (1994).
[11] S. Porowski and I. Grzegory, in *Properties of Group III Nitrides*, edited by J. H. Edgar (INSPEC, IEE, London, 1994).
[12] G. L Doll, in Ref. 11.
[13] A. F. Wright and J. S. Nelson, Phys. Rev. B **50**, 2159 (1994); **51**, 7866 (1995).
[14] T. Azuhata, T. Sota, K. Suzuki, and S. Nakamura, J. Phys.: Condens. Matter **7**, L129 (1995).
[15] G. Capellini, V. Fiorentini, K. Tenelsen, and F. Bechstedt, in *Gallium Nitrite and Related Materials*, edited by R. D. Dupuis *et al.*, MRS Symposia Proceedings No. 395 (Materials Research Society, Pittsburgh, 1996), p. 429.
[16] M. Ferhat, A. Zaoui, M. Certier, and H. Aourag, Physica B **252**, 229 (1998).
[17] R. Miotto, G. P. Srivastava, and A. C. Ferraz, Surf. Sci. **426**, 75 (1999).
[18] R. Miotto, G. P. Srivastyava, and A. C. Ferraz, Surf. Sci. **433**, 377 (1999).
[19] R. Miotto, A. C. Ferraz, and G. P. Srivastava, Solid State Commun. **115**, 67 (2000).
[20] K. Karch and F. Bechstedt, Phys. Rev. B **56**, 7404 (1997).
[21] K. Karch, J. M. Wagner, and F. Bechstedt, Phys. Rev. B **57**, 7043 (1998).
[22] J. M. Wanger and F. Bechstedt, Phys. Status Solidi B **216**, 793 (1999).
[23] T. Pletl, P. Pavone, U. Engel, and D. Strauch, Physica B **263**, 392 (1999).
[24] F. Bechstedt, U. Grossner, and J. Furthmüller, Phys. Rev. B **62**, 8003 (2000).
[25] C. Bungaro, K. Rapcewicz, and J. Bernholc, Phys. Rev. B **61**, 6720 (2000).
[26] H. M. Tütüncü and G. P. Srivastava, Phys. Rev. B **62**, 5028 (2000).
[27] S. Duman, Master thesis, University of Sakarya in Turkey, 2002.
[28] A. Gingolani, M. Ferrara, M. Lugara, and G. Scamario, Solid State Commun. **58**, 823 (1986).
[29] L. Filippidis, H. Siegle, A. Hoffmann, C. Thomsen, K. Karch, and F. Bechstedt, Phys. Status Solidi B **198**, 621 (1996).
[30] A. Tabata, R. Enderlein, J. R. Leite, S. W. da Silva, J. C. Galzerani, D. Schikora, M. Kloidt, and K. Lischka, J. Appl. Phys. **79**, 4137 (1996).
[31] A. Cros, R. Dimitrov, H. Ambacher, M. Stuzmann, S. Christiansen, M. Albrecht, and H. P. Strunk, J. Cryst. Growth **181**, 197 (1997).
[32] V. Yu. Davydov, Yu. E. Kitaev, I. N. Goncharuk, A. N. Smirnov, J. Graul, O. Semchinova, D. Uffmann, M. B. Smirnov, A. P. Mirgorodsky, and R. A. Evarestov, Phys. Rev. B **58**, 12 899 (1998).
[33] H. Harima, T. Inoue, S. Nakashima, H. Okumura, Y. Ishida, S. Yoshida, T. Koizumi, H. Grille, and F. Bechstedt, Appl. Phys. Lett. **74**, 191 (1999).
[34] M. Schwoerer-Bohning, A. T. Macrander, M. Pabst, and P. Pavone, Phys. Status Solidi B **215**, 177 (1999).
[35] T. Ruf, J. Serrano, M. Cardona, P. Pavone, M. Pabst, M. Krisch, M. D'Astuto, T. Suski, I. Grzegory, and M. Leszczynski, Phys. Rev. Lett. **86**, 906 (2001).
[36] C. A. Swarts, T. C. McGill, and W. A. Goddard III, Surf. Sci. **110**, 400 (1981).
[37] X. J. Chen, J. M. Langlois, and W. A. Goddard III, Phys. Rev. B **52**, 2348 (1995).
[38] J. E. Jaffe, R. Pandey, and P. Zapol, Phys. Rev. B **53**, R4209 (1996).
[39] P. Zapol, R. Pandey, and J. D. Gale, J. Phys.: Condens. Matter **9**, 9517 (1997).
[40] U. Grossner, J. Furthmüller, and F. Bechstedt, Phys. Rev. B **58**, R1722 (1998).
[41] B. K. Agrawal, P. Srivastava, and S. Agrawal, Surf. Sci. **405**, 54 (1998).
[42] H. M. Tütüncü, R. Miotto, G. P. Srivastava, and J. S. Tse, Phys. Rev. B **66**, 115304 (2002).
[43] N. Troullier and J. L. Martins, Phys. Rev. B **43**, 1993 (1991).
[44] J. P. Perdew, K. Burke, and M. Ernzerhof, Phys. Rev. Lett. **77**, 3865 (1996).
[45] S. Baroni, P. Giannozzi, and A. Testa, Phys. Rev. Lett. **58**, 1861 (1987).
[46] S. Baroni, S. de Gironcoli, A. Dal. Corso, and P. Giannozzi, Rev. Mod. Phys. **73**, 515 (2000).
[47] F. D. Murnaghan, Proc. Natl. Acad. Sci. U.S.A. **50**, 697 (1944).
[48] G. P. Srivastava, *Theoretical Modelling of Semiconductor Surfaces* (World Scientific, Singapore, 1999).
[49] C. B. Duke, Appl. Surf. Sci. **65**, 543 (1993).
[50] H. M. Tütüncü and G. P. Srivastava, J. Phys. Chem. Solids **58**, 685 (1997).
[51] J. Fritsch and U. Schröder, Phys. Rep. **309**, 209 (1999).
[52] J. Fritsch, P. Pavone, and U. Schröder, Phys. Rev. Lett. **71**, 4194 (1993).
[53] H. M. Tütüncü and G. P. Srivastava, J. Phys.: Condens. Matter **8**, 1345 (1996).
[54] H. M. Tütüncü, S. Bağci, S. Duman, and G. P. Srivastava, Phys. Status Solidi C **1**, 3023 (2004).